Journal of Power Sources 195 (2010) 7524–7529

Contents lists available at ScienceDirect

Journal of Power Sources

journal homepage: www.elsevier.com/locate/jpowsour

Electrochemical behavior of negative electrode of lead-acid cells based on reticulated vitreous carbon carrier

A. Czerwiński[a,b], S. Obrębowski[a,b], J. Kotowski[b], Z. Rogulski[a,b,*], J.M. Skowroński[c], P. Krawczyk[c], T. Rozmanowski[c], M. Bajsert[d], M. Przystałowski[d], M. Buczkowska-Biniecka[d], E. Jankowska[e], M. Baraniak[e]

[a] Instytut Chemii Przemysłowej, ul. Rydygiera 8, 01-793 Warszawa, Poland
[b] Warsaw University, Departament of Chemistry, ul. Pasteura 1, 02-093 Warszawa, Poland
[c] Poznań University of Technology, ul. Piotrowo 3, 60-965 Poznań, Poland
[d] JENOX Ltd., ul. Notecka 33, 61-800 Chodzież, Poland
[e] IMN Central Laboratory of Cells and Batteries, ul. Forteczna 14, 61-362 Poznań, Poland

ARTICLE INFO

Article history:
Received 4 September 2009
Received in revised form
11 December 2009
Accepted 14 December 2009
Available online 21 December 2009

Keywords:
Lead-acid cell
Negative electrode
Electrode carrier
Reticulated vitreous carbon
Cyclic voltammetry
Discharge/charge reversibility

ABSTRACT

Reticulated vitreous carbon (RVC®) and RVC® plated with lead were investigated as carriers for the negative electrode of lead-acid cell. The RVC® and Pb/RVC® carriers were pasted with active paste (received from JENOX Ltd., Polish producer of lead-acid batteries) and prepared to be used in lead-acid cell. Comparative study of electrodes based on RVC® and Pb/RVC® has been done using constant-current charging/discharging, constant-potential discharging and cycling voltammetry measurements. Scanning electron microscopy (SEM) was employed to determine the morphology of the lead layer deposited on the RVC surface. Hybrid flooded single lead-acid cells containing one negative electrode, based on new type of carrier (RVC® or Pb/RVC®), sandwiched between two positive electrodes, based on the Pb–Ca grids, were assembled and subjected to electrochemical tests. It has been found that both materials, RVC® and Pb/RVC®, can be used as carriers of negative electrode, but the latter seems to have better influence on the discharge performance.

1. Introduction

During the past 150 years, the construction of a lead-acid battery (LAB) has changed significantly but in comparison to other rechargeable batteries (i.e. nickel–metal hydrides or lithium-ion batteries) the main disadvantage of a classic lead-acid battery still remains its low mass energy density mainly due to high mass of lead-based carriers into which the electrochemically active mass is inserted [1–3]. Preliminary laboratory tests have proved that carrier and current collectors reticulated vitreous carbon seem to be very promising in this respect, but many difficulties have to be dissolved before applying them in lead-acid batteries [4,5].

In our study reticulated vitreous carbon (RVC®) has been chosen as a carrier for negative electrodes of LAB. RVC® is an inexpensive and chemically inert carbon material characterized by an open pore structure and highly developed surface [6–8]. It has been widely applied as an electrode material, including the use as a substrate for deposition of various metals. Due to its unique properties RVC® is attractive for electrochemical studies and can be regarded as an electrode carrier applicable to energy storage systems [9].

The idea of lead-acid battery construction with carbon as a carrier–collector made of RVC® has been proposed and described by Czerwiński [10], who since 1995, has reported the results in several patents [11,12] and papers [4,5,13]. RVC® being the porous glassy carbon was modified by coating with thin layer of pure lead (Pb/RVC®). The Pb/RVC® electrodes are supposed to exhibit almost identical electrochemical behavior to pure metallic lead. Gyenge et al. [14,15] have adapted this invention in the construction of a new type of lead-acid rechargeable cell where RVC® coated with lead-based alloys was used as a carrier for active mass in the negative electrode. Application of graphite as an electrode material in LAB has been studied by Das and Mondal [16–18]. A very interesting conception of carrier based on carbon has been demonstrated by Chen et al. [19–22] who used pitch-based carbon foam which is different material than the RVC (obtained by the pyrolysis of phenolics) but resemble similar morphology. Kao et al. [23] have found out that after coating the lead grid with barium metaplumbate (BMP)

* Corresponding author at: Industrial Chemistry Research Institute, Rydygiera 8, 01-793 Warsaw, Poland. Tel.: +48 22 568 2447; fax: +48 22 569 2390.
E-mail address: zbigniew.rogulski@ichp.pl (Z. Rogulski).

0378-7753/$ – see front matter © 2009 Elsevier B.V. All rights reserved.
doi:10.1016/j.jpowsour.2009.12.051

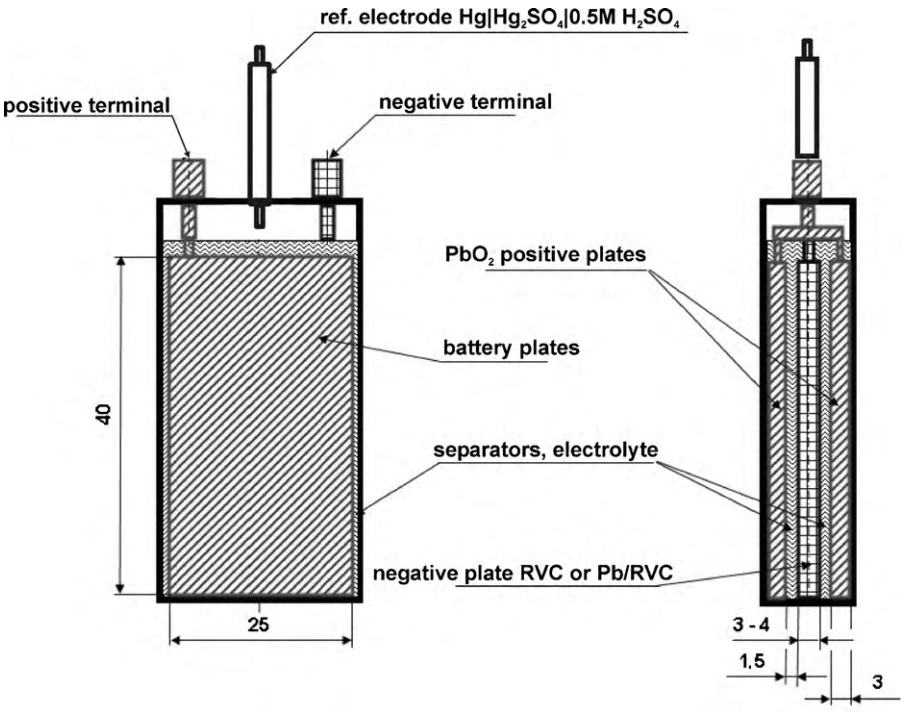

Fig. 1. Scheme of three electrode lead-acid electrode cell for negative plate testing.

and a layer of lead corrosion resistance of positive lead-acid battery electrode has improved significantly. Also additives of BMP into positive plates improve the performance of lead-acid battery [24]. The cyclic voltammogram obtained for lead deposited on BMP [25] is generally similar to CV of lead deposited on RVC® [4]. Only the "anodic excursion" peak, which usually appears as a result of cracking of the lead layer [26] is not observed. This is probably due to different morphologies of deposits.

In this paper the electrochemical characteristics and performance of negative electrode with new type of carrier/collector are demonstrated in the lead-acid cell. In our experimental lead-acid cells RVC® or Pb/RVC® material have been used as both negative active mass (NAM) carrier and negative plate current collector.

2. Experimental

RVC of 20 p.p.i. (pores per inch) porosity grade, made by ERG, Material and Aerospace Corporation, has been used as the negative electrode carrier. The average dimensions of RVC® plate were 40 mm × 25 mm × 3 mm. The negative electrode was prepared from the original RVC® and RVC® plated with thin layer of lead (10–15 μm). Thickness of Pb layer was calculated basing on Pb deposit weight and the real surface area of used RVC [27] (manufacturer data). Morphologies of the RVC® and Pb surfaces were examined with a LEO 435VP scanning electron microscope (SEM). Uncovered RVC® and that covered with lead were pasted with negative active mass usually used by JENOX Ltd. in SLI lead-acid batteries. Negative mass is composed of lead powder, lead oxides, sulfuric acid, expanders and other additives. Electrical contact made of a bundle of thin Pb wires (0.5 mm in diameter) was attached to the RVC carrier. The average weight of the lead-coated RVC carrier together with electrical contact, ranging between 1.4 g and 1.6 g, was ca. 12% of total active mass introduced into porous Pb/RVC® matrix. The weight of pure RVC plate was between 0.14 g and 0.16 g. The next step of electrode production was curing the electrodes (RVC carrier filled with active mass) in air (45 °C, 90% relative humidity) and drying in 45 °C at ambient humidity. The amount of lead in dry negative mass was 88.5%.

After curing, the electrodes were soaked with H_2SO_4 electrolyte ($d = 1.16\,g\,cm^{-3}$) and electroformed at current of 100 mA. The details related to the preparation of negative electrodes are described in a separate paper [28]. The amount of active mass in dry plates after preparation process was in the range 11.0–15.0 g (±0.5 g). Hybrid single cell lead-acid batteries composed of one negative plate, based on a new type of carrier (RVC or Pb/RVC), sandwiched between two positive electrodes, based on the Pb–Ca grids, were assembled and subjected to electrochemical tests (Fig. 1). Positive plates used to construct the cell were donated by JENOX (from traction lead-acid battery; 60 Ah, 12 V). The geometric area of positive electrodes was similar to the RVC-based negative ones, i.e. 40 mm × 25 mm × 3 mm. The amount of the active mass in the positive plates was in excess compared with the amount of active mass in the negative electrode to ensure complete reaction in the latter. Typical polyethylene separator usually used in SLI lead-acid batteries was used. The cell was filled with electrolyte (36% H_2SO_4). Electrochemical characterization of negative electrodes was performed using a three electrode system where the positive plates played a role of auxiliary electrodes, whereas the $Hg/Hg_2SO_4/1\,M\ H_2SO_4$ electrode, inserted into the cell shown in Fig. 1, was used as the reference electrode.

For characterization of RVC/Pb carrier the cyclic voltammetric measurements (CV) were made in the potential range of −1.5 V to 1.6 V using a scan rate of $10\,mV\,s^{-1}$ whereas CV measurements of the negative electrodes (completed lead-acid negative plates) were carried out in the range potentials between −1.15 V and −0.60 V at a scan rate $0.02\,mV\,s^{-1}$. CV measurements of the negative electrode were started at the rest potential of electrodes ($E_R = -1.04$ V) and the potential was changed towards less negative values (anodic polarization/discharging) to reach the value of −0.60 V and after the reversal of polarization direction the potential decreased (cathodic polarization/charging) to the value of −1.15 V was attained. Before starting the CV measurements the negative electrodes were subjected to galvanostatic charging in experimen-

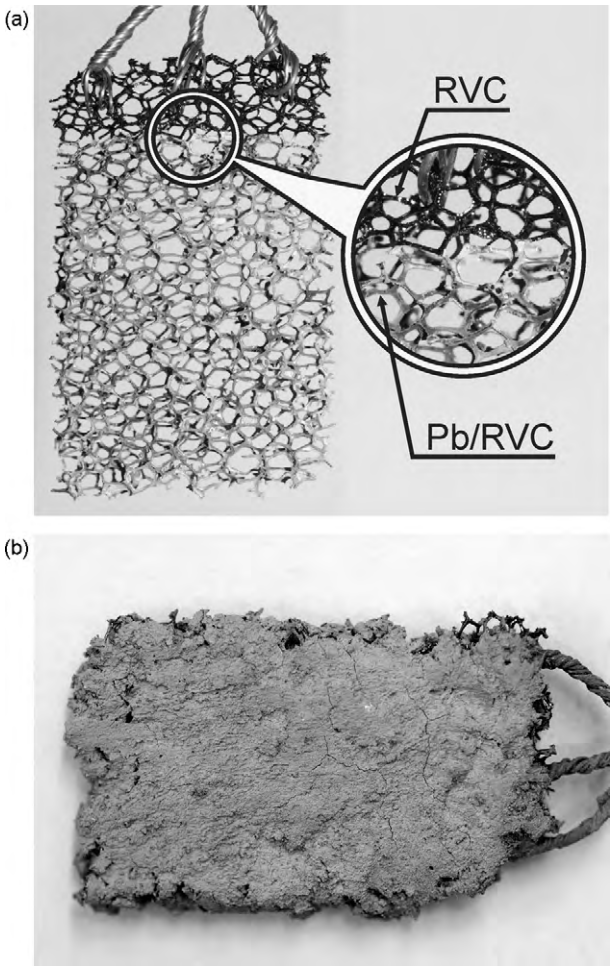

Fig. 2. (a) RVC carrier–collector covered with lead. (b) RVC based lead-acid negative electrode.

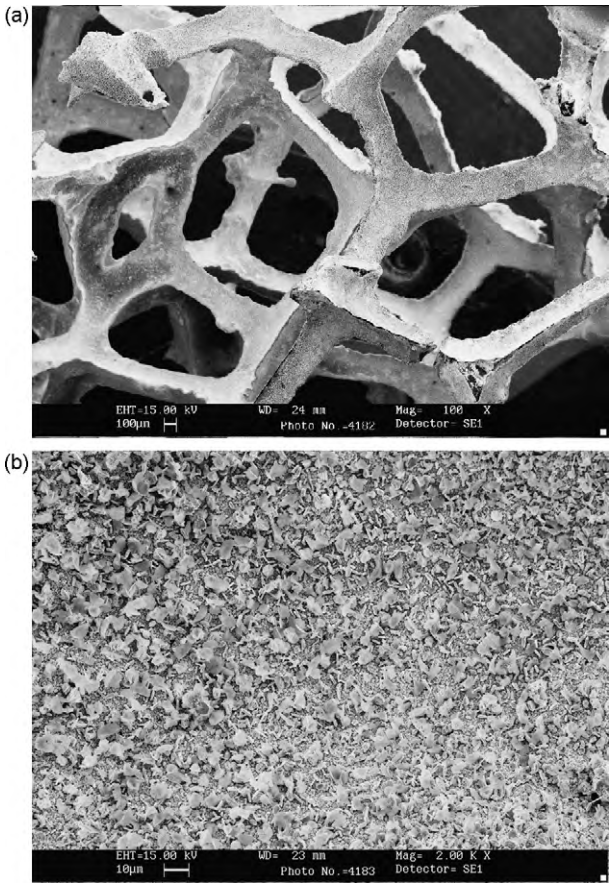

Fig. 3. (a) SEM image of Pb/RVC carrier magnification 100×. (b) SEM image of Pb deposited on RVC, magnification 2000×.

tal lead-acid cell (Fig. 1) at a rate of 0.05*C* (*C*—nominal capacity) and the nominal capacity was estimated at the level of 1.5–2.2 Ah per cell, dependent on the amount of active mass (150 mAh per 1 g of active mass).

Constant-current charging/discharging runs of negative electrodes were carried out at 0.1*C* and cut-off at −1.30 V and −0.75 V, respectively.

Discharging of the negative electrodes at the constant-potential was performed at the potential −0.95 V for 240 s.

The changes of the electrode potential were also recorded during the pulse constant-current discharge measurements. The time of pulse was 120 s. Starting at a pulse current of 10 mA, the current value was gradually increased.

All electrochemical measurements were made at a room temperature using AutoLab PGSTAT-30 potentiostat–galvanostat. A saturated mercury sulfate electrode $Hg|Hg_2SO_4|0.5\,M\ H_2SO_4$ (SMSE) was used as the reference electrode.

3. Results

3.1. Morphology and electrochemical properties of Pb/RVC carriers

Fig. 2a shows the picture of Pb/RVC carrier of negative electrode (RVC coated with thin layer of lead; 10–20 μm) [29,30] with connected Pb wires, whereas the negative electrode obtained by pasting Pb/RVC® with active mass and curing is depicted Fig. 2b. The thickness of the negative plate after preparation was 3–4 mm. Fig. 3a and b presents SEM images of Pb/RVC® electrode recorded at different magnifications of 100× and 2000×, respectively. Fig. 3b demonstrates that the carbon surface is tightly covered with homogeneous Pb layer. Pb layer has solid, continuous structure without cracks over whole RVC® surface. This layer prevents active mass from contact with the carbon surface of RVC® after pasting the electrode.

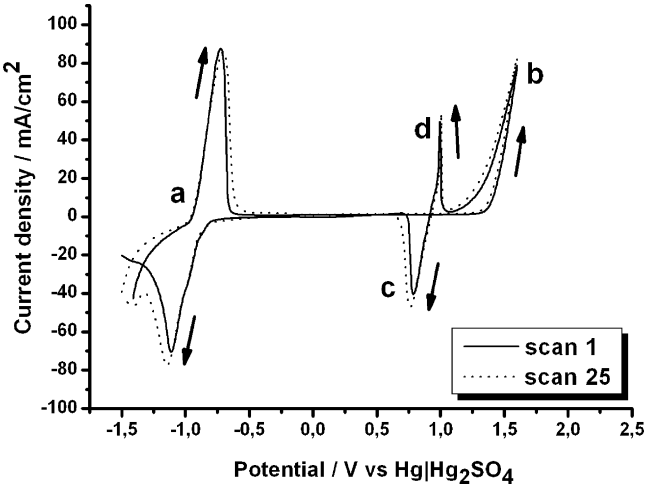

Fig. 4. Cyclic voltammograms in 0.5 M H_2SO_4 of the Pb layer deposited on RVC. Polarization speed 10 mV s^{-1} and Pb layer thickness 15 μm.

Fig. 4 presents CV curves for Pb layer deposited on RVC® (Pb/RVC® carrier). The main redox processes of the lead electrode are as follows: (a) the reduction of Pb(II) to metallic Pb and subsequent oxidation to Pb(II) which occurs at highly negative potentials in the potential range from −1.4 V to 0.6 V and (b) the oxidation of Pb (II) to Pb (IV) seen at highly positive potentials ca. +1.5 V. The shape of these peaks does not change significantly with the concentration of sulfuric acid. This is contrary to the main reduction peak (c) occurring at potential close to +0.8 V. Moreover, this peak is usually associated with oxidation current (d) which is visible as anodic peak (in the literature called "anodic excursion") [26,31]. According to earlier suggestions [26], cracks which were formed on the electrode surface due to a significant difference between molar volumes of α-PbO_2 and $PbSO_4$ (Pb(IV) → Pb(II)) are responsible for this effect. Exposed fresh lead (under cracks) is oxidized and this reaction is responsible for "excursion peak". The lead oxidation currents overlap with currents of PbO_2 reduction process and both processes occur simultaneously on the electrode. The details about such a behavior of lead electrode were described and discussed earlier [31]. In Fig. 4 one can notice that the shape of CV curves does not change during cyclic polarization of Pb/RVC® electrode. It proves that the deposited layer of Pb on RVC is stable in cyclic electrochemical treatment.

3.2. Electrochemical characteristics of negative electrodes based on RVC and Pb/RVC carriers

Fig. 5 presents the plots obtained during typical procedure of constant-current charging/discharging ($Pb + HSO_4^{2-}$ $\underset{\text{charging}}{\overset{\text{discharging}}{\rightleftarrows}}$ $PbSO_4 + H^+ + 2e$) runs of negative electrodes carried out at 0.1*C* and cut-off at −1.30 V and −0.75 V, respectively. Fig. 5a refers to negative electrode with RVC carrier, whereas Fig. 5b relates to negative electrode with Pb/RVC® carrier. Before these experiments the complete cell was five times deeply charged and discharged to the voltage of 1.75 V and the density of electrical capacity of the negative electrode was estimated at a rate 0.05*C* (80 mA of discharging current). Specific weight capacities of active mass, estimated from the constant-current charging/discharging measurements, deposited in RVC® and Pb/RVC® carriers are close to each other and equal to 0.146 Ah g^{-1} and 0.141 Ah g^{-1}, respectively. The charging process was cut-off at −1.30 V, whereas discharging process was stopped at −0.75 V. The specific capacity of negative electrode, estimate based on the charging/discharging measurements with the used current of 0.16 A (corresponding to the rate around 0.1*C*) was equal to 0.118 Ah g^{-1} (RVC®) and 0.102 Ah g^{-1} (Pb/RVC®), whereas the discharge/charge efficiency of the electrodes in constructed lead-acid cell was 0.99. This value is acceptable for lead-acid batteries under conditions of the constant-current discharging at a rate 0.05*C* [1,3]. In Fig. 5 one can observe two plateaus on charging curves recorded under constant-current measurements. The former appears at higher potential after starting the discharging process and after some time of charging descend to a new plateau at lower potential. (From comparison of) Comparing Fig. 5a and b one can see that the plateau at high potential is markedly longer for electrode containing RVC® carrier coated with the Pb layer (Fig. 5b)

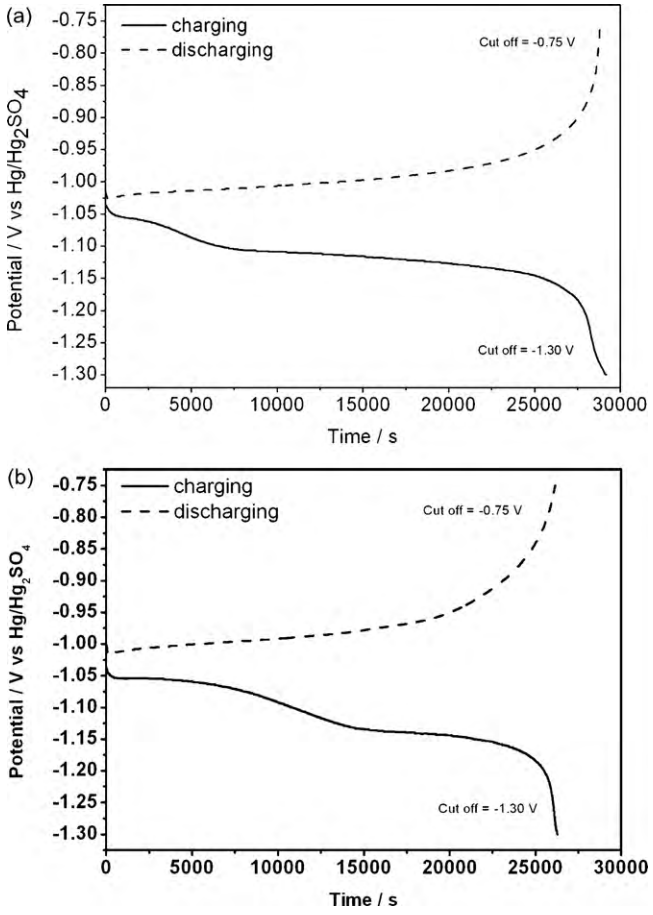

Fig. 5. Potential–time characteristics recorded during the constant-current charging/discharging process for negative electrode based on RVC (a) and Pb/RVC (b) carrier.

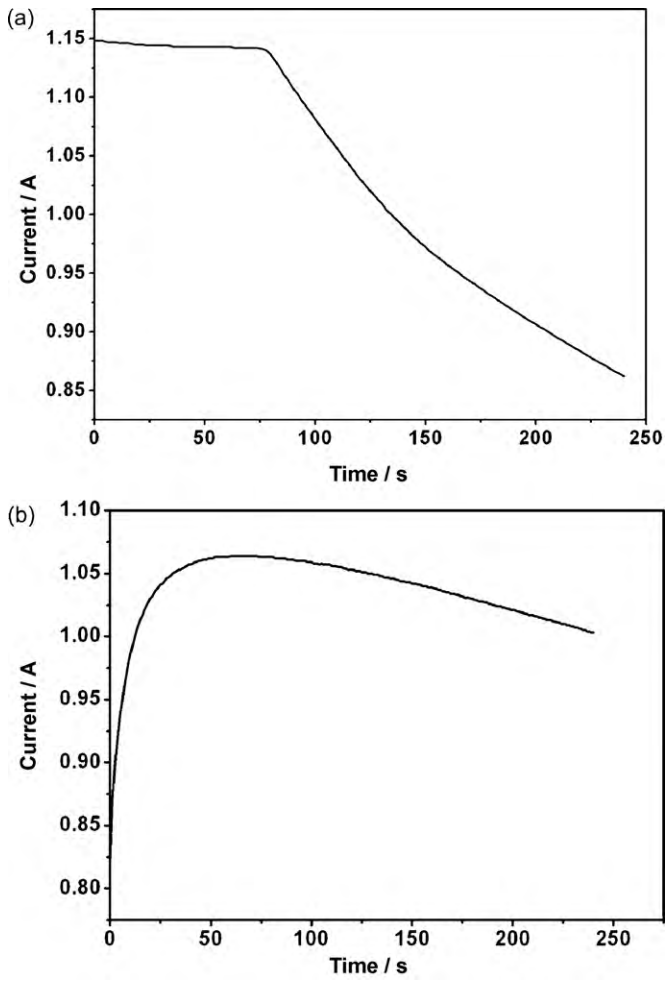

Fig. 6. Constant-potential discharging curves for charged negative electrodes based on RVC (a) and Pb/RVC (b) carrier. Discharge potential: −0.95 V. Total time of discharging: 240 s.

than for electrode with uncoated RVC® carrier (Fig. 5a). Such a behavior indicates the existence of at least two paths of charging process taking part inside the negative electrode. The result obtained leads to the conclusion that the mechanism of the process is strongly modified by the presence of Pb layer on the RVC® surface. We should also take into account the hydrogen evolution process during the charging process of negative plate with bare RVC carrier. The overvoltage of hydrogen evolution on carbon electrode is much lower in comparison to the same process on lead. This process can have the influence on the shape of the demonstrated plots.

The influence of Pb layer is clearly reflected in the discharging process performed in the potentiostatic mode at the potential −0.95 V. Similar to Fig. 5, two distinct regions are also observed on the current–time discharging curves presented in Fig. 6. These curves differ considerably in shape depending on whether RVC® is coated with Pb or not. For the electrode containing RVC® carrier (Fig. 6a) the first region is recorded at high current (ca. 1.15 A) after the beginning of the discharging process. This region is flat and very short. After passing the charge of ca. 100–110*C* the curve descends abruptly with time. Such a behavior being consistent with the conclusion drawn based on Fig. 5 indicates the existence of at least two steps of charging/discharging processes taking part inside the negative plate. These effects can be explained by the fact that on RVC® matrix the rate and/or mechanism of Pb redox processes ($Pb \leftrightarrow PbSO_4$) differs from the same charging/discharging reaction in the bulk of active mass. It was found that even electrodes which after long time of cycling performance lost the electrical capacity also show above behavior. It supports the hypothesis that $Pb \leftrightarrow PbSO_4$ processes on RVC® matrix are responsible for this effect. The shape of the *I*–*t* plot obtained for negative electrode with Pb/RVC® carrier (Fig. 6b) differs significantly in comparison with the electrode containing RVC® carrier (Fig. 6a). For Pb/RVC based electrode polarization during the first 50 s the *I*–*t* curve rises. This increase of current value is likely associated with the effect of simultaneous reactions occurring inside the bulk of active mass and at the active mass/lead/RVC® interface. This effect is stronger for Pb/RVC® based electrode than in the electrode based on RVC® not covered with lead. It is worth noting that the discharge current recorded for the electrode with Pb/RVC® is significantly higher in comparison with the electrode with the original RVC® carrier. Also the drop of the discharge current value with time is significantly lower for Pb/RVC® electrode than for that with the original RVC®. The results obtained allow the expectation that the performance of negative electrode based on Pb/RVC® carrier in lead-acid battery will be better.

Cyclic voltammograms for negative electrodes of lead-acid cell based on RVC® and Pb/RVC® carrier are presented in Fig. 7. The charges calculated from the anodic peaks in the first sweep are equal to 0.125 Ah g^{-1} and 0.107 Ah g^{-1} for electrodes with RVC® (Fig. 7a) and Pb/RVC® (Fig. 7b) carriers, respectively. These values are close to those obtained at the constant-current discharging at a rate of 0.1*C* (see Fig. 5). It can be expected that during the elec-

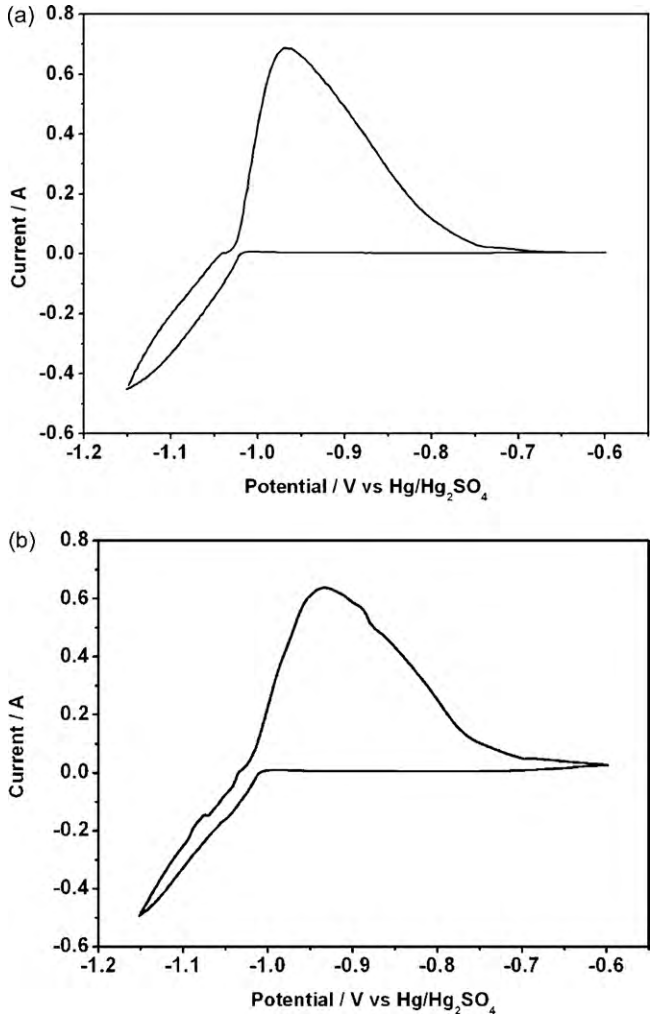

Fig. 7. Cyclic voltammograms recorded during the first cycle for the negative electrode based on RVC (a) and Pb/RVC (b) carrier. Scan rate: 0.02 mV s^{-1}. Potential scanning: $E_R = -1.04\,V \rightarrow -0.60\,V \rightarrow -1.15\,V \rightarrow -0.60\,V \rightarrow -1.04\,V$.

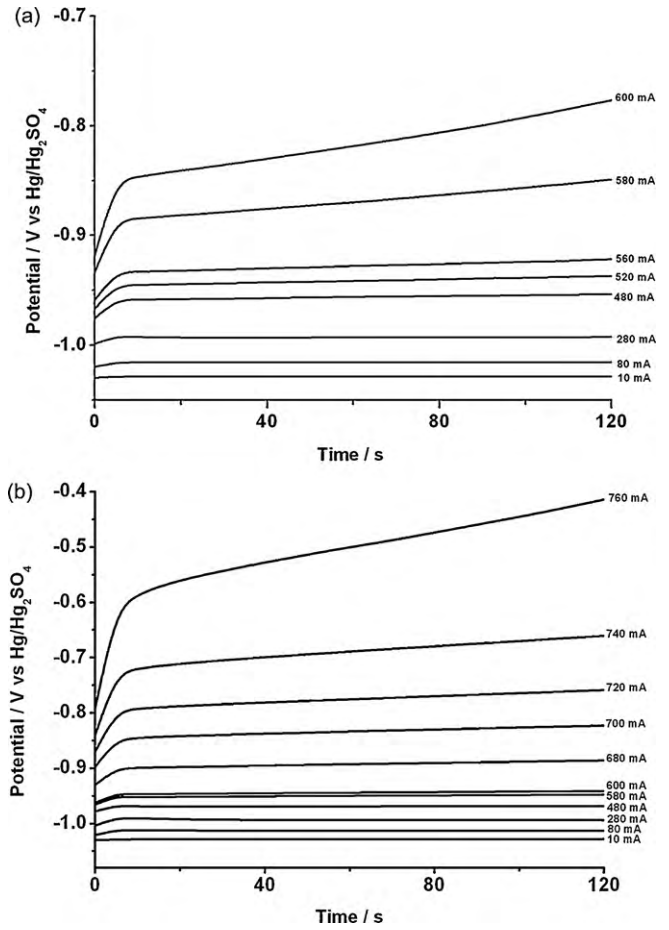

Fig. 8. The *E*–*t* curves recorded during the constant-current discharging pulses for the negative electrode based on RVC (a) and Pb/RVC (b) carrier. Time of current pulse: 120 s.

troformation process of negative electrode porous layer of lead is deposited on RVC® or Pb/RVC® carriers. This additional layer of porous lead on the carrier surface influences also electrochemical behavior of negative electrodes. One can recognize the difference between the shapes of the voltammograms of the electrodes with RVC® (Fig. 7a) and Pb/RVC® (Fig. 7b) carrier. Particularly interesting features are observed on the anodic/discharging peak. For RVC® based electrode one asymmetric peak is noted. On starting the potential scanning the rapid increase of anodic current is observed to reach the maximum at about −0.97 V and then the current line descends more gently and its slope is very smooth. In contrast to such a feature, the current maximum for the electrode with Pb/RVC® (Fig. 7b) is shifted ca. 50 mV towards less negative potentials and a small kink appears at −0.83 V followed by a broad shoulder at −0.83 V. Such a shape of the peak can arise from overlapping two peaks. In the light of this, it is reasonable to assume that a two-phase process occurs for Pb/RVC® based electrode, probably associated with the existence of Pb layer on the carbon surface. This explanation is in agreement with the suggestion derived based on an interpretation of the *I*–*t* curves depicted in Fig. 6. The plots obtained in the discharge measurements using the pulse current–time technique are shown in Fig. 8. As mentioned in Section 2, after imposing each current pulse, increasing step by step from the initial value of 10 mA, onto the negative electrode the potential response was recorded for 120 s. For electrode based on the original RVC the significant potential changes were not observed up to 580 mA of discharging current. A dramatic polarization of electrode potential took place at 600 mA of discharging current. For electrode with Pb/RVC® carrier the electrode polarization was not observed up to 740 mA of discharging current. A significant polarization was observed at 760 mA. These results indicate clearly that negative electrodes of lead-acid cell with Pb/RVC® carrier are more resistive to a high current polarization.

4. Conclusions

The influence of RVC and Pb/RVC® carrier on electrochemical behavior of negative electrodes in lead-acid cells has been observed. It seems that the differences in interaction between carrier and active mass are due to the presence of thin layer of lead on the surface of RVC®. It has been suggested that during the formation process of negative electrodes the porous layer of lead is deposited on both carriers, i.e. on RVC or Pb/RVC®. This additional layer of porous lead deposited on matrix RVC® or Pb/RVC® substrate during the cell formation influences also electrochemical behavior of negative electrodes. The differences in the influence of carrier composition on electrochemical behavior of negative electrodes are significantly reflected in the constant-potential and constant-current slopes. The application of RVC® carrier in lead-acid batteries decreases to ca. 10% of the carrier and collector participation in the electrode weight. Moreover, the structure of RVC® leads to better electrical conductivity in the whole bulk of active mass deposited on/in matrix. It is proved by the obtained high density of charge capacity of active mass in negative plates (ca.150 Ah kg^{-1}). The results prove that both used carriers RVC® and Pb/RVC® can be used as a carrier in negative electrodes of lead-acid cell although the latter carrier exhibits better behavior during the discharging performance at high currents and better durability under high current pulse discharging. We cannot exclude that the evolution of hydrogen on bare RVC (lower overpotential on carbon than on lead) has important influence on electrochemical behavior of negative plate and this reaction can be the reason why the electrode with Pb/RVC has better durability under high current treatment.

Acknowledgements

This work was partially supported by the Ministry of Scientific Research and Information Technology – project no. R001/01/06, Warsaw University and Industrial Chemistry Research Institute in Warsaw.

References

[1] D. Linden, T.B. Reddy, Handbook of Batteries, McGraw-Hill, New York, 1993.
[2] M. Barak (Ed.), Electrochemical Power Sources, The Institution of Electrical Engineers, London and New York Peter Peregrinus Ltd., Stevenage, UK and New York, 1980.
[3] D.A.J. Rand, P.T. Moseley, J. Garche, C.D. Parker (Eds.), Valve-regulated Lead-acid Batteries, Elsevier, 2004.
[4] A. Czerwiński, M. Żelazowska, J. Electroanal. Chem. 410 (1996) 53–60.
[5] A. Czerwiński, M. Żelazowska, J. Power Sources 64 (1997) 29–34.
[6] J. Wang, Electrochim. Acta 26 (1981) 1721–1726.
[7] J.M. Friedrich, C. Ponce-de-Leon, G.W. Reade, F.C. Walsh, J. Electroanal. Chem. 561 (2004) 203–217.
[8] Z. Rogulski, W. Lewdorowicz, W. Tokarz, A. Czerwinski, Polish J. Chem. 78 (2004) 1357–1370.
[9] A. Czerwiński, Z. Rogulski, H. Siwek, S. Obrębowski, I. Paleska, M. Chotkowski, M. Łukaszewski, J. Appl. Electrochem. 39 (2009) 559–567.
[10] A. Czerwiński, Patent RP 167,796 (1995).
[11] A. Czerwiński, M. Żelazowska, Patent RP 178,258 (2000).
[12] A. Czerwiński, M. Żelazowska, Patent RP 180,939 (2001).
[13] A. Czerwiński, Conf. Proc. LABAT 96, Varna, Bulgaria, 1996, pp. 107–110.
[14] E. Gyenge, J. Jung, B. Mahato, J. Power Sources 113 (2003) 388–395.
[15] E. Gyenge, J. Jung, Patent No. WO03028130.
[16] K. Das, A. Mondal, J. Power Sources 35 (1995) 251–254.
[17] K. Das, A. Mondal, J. Power Sources 89 (2000) 112–116.
[18] K. Das, A. Mondal, Trans. SAEST, 36, J. Power Sources No. 1 & 2 (January–June 2001).
[19] L.W. Ma, B.Z. Chen, Y. Chen, Y. Yuan, J. Appl. Electrochem. 39 (2009) 1609–1615.
[20] Y. Chen, B.-Z. Chen, L.W. Ma, Y. Yuan, J. Appl. Electrochem. 38 (2008) 1409–1413.
[21] Y. Chen, B.Z. Chen, L.W. Ma, Y. Yuan, Electrochem. Commun. 10 (2008) 1064–1066.
[22] Y. Chen, B.Z. Chen, X.C. Shi, H. Xu, W. Shang, Y. Yuan, L.P. Xiao, Electrochim. Acta 53 (2008) 2245–2249.
[23] W.H. Kao, S.L. Haberichter, K. Bullock, J. Electrochem. Soc. 139 (1992) L105–L107.
[24] W.H. Kao, S.L. Haberichter, P. Patel, J. Electrochem. Soc. 141 (1994) 3300–3305.
[25] I. Paleska, R. Pruszkowska-Drachal, J. Kotowski, Z. Rogulski, J.D. Milewski, Czerwiński, J. Power Sources 129 (2004) 326–329.
[26] R.L. Deutscher, S. Fletcher, J.A. Hamilton, J. Electroanal. Chem. 31 (1986) 585–589.
[27] ERG Materials and Aerospace Corporation, Duocel® Foam Properties, http://www.ergaerospace.com/foamproperties/introduction.htm.
[28] A. Czerwiński, S. Obrębowski, J. Kotowski, Z. Rogulski, J.M. Skowroński, M. Bajsert, M. Przystałowski, M. Buczkowska-Biniecka, E. Jankowska, M. Baraniak, J. Rotnicki, M. Kopczyk, J. Power Sources 195 (2010) 7530–7534.
[29] A. Czerwiński, S. Obrębowski, J. Kotowski, M. Bajsert, M. Przystałowski, Patent pending P-387975 (2009).
[30] A. Czerwiński, S. Obrębowski, J. Kotowski, M. Bajsert, M. Przystałowski, Patent pending P-387976 (2009).
[31] A. Czerwiński, M. Żelazowska, M. Grdeń, K. Kuc, J.D. Milewski, A. Nowacki, G. Wójcik, M. Kopczyk, J. Power Sources 85 (2000) 50–56.